Full Paper

Applied Organometallic Chemistry

Received: 18 August 2013 Revised: 11 October 2013 Accepted: 29 October 2013 Published online in Wiley Online Library: 21 January 2014

(wileyonlinelibrary.com) DOI 10.1002/aoc.3104

DNA binding and antibacterial properties of ternary lanthanide complexes with salicylic acid and phenanthroline

Bin Yue, Hui-Juan Sun, Ying-Nan Chen, Kai Kong, Hai-Bin Chu and Yong-Liang Zhao*

Twelve ternary lanthanide complexes RE(sal)$_3$phen (RE^{3+} = La^{3+}, Pr^{3+}, Nd^{3+}, Sm^{3+}, Eu^{3+}, Gd^{3+}, Tb^{3+}, Dy^{3+}, Ho^{3+}, Tm^{3+}, Yb^{3+}, Lu^{3+}, sal = salicylic acid, phen = phenanthroline) were prepared. Interactions between the complexes and calf thymus DNA (ct-DNA) were investigated using UV–visible spectrophotometry, fluorescence quench experiment and viscosity measurement. Hypochromicity and red shift of the absorption spectra of complexes were observed in the presence of DNA. The enhanced emission intensity of ethidium bromide (EB) in the presence of DNA was quenched by the addition of lanthanide complexes, which indicated that the lanthanide complexes displaced EB from its binding sites in DNA. Based on the systematic research of the binding constant (K_b) and the fluorescence quenching constant (K_q) of the 12 complexes, we found that the complexes with smaller lanthanide ion radius had stronger binding abilities with DNA. Viscosity measurement showed that the relative viscosity of the DNA solution was enhanced with increasing the amounts of the complexes. All these results suggested that the complexes could bind to DNA and the major binding mode was intercalative binding. Moreover, all these complexes exhibited excellent antibacterial abilities against *Escherichia coli*. Also, the antibacterial activities of complexes with heavy rare earth were higher than those of complexes with light rare earth. Copyright © 2014 John Wiley & Sons, Ltd.

Additional supporting information may be found in the online version of this article at the publisher's web-site.

Keywords: lanthanide complexes; ct-DNA; fluorescence quenching; binding mode; antibacterial activity

Introduction

Owing to the potential applications of metal complexes as anticancer drugs with other biological functions,[1–5] the interactions of metal complexes with nucleic acids have aroused tremendous interests in recent years.[6,7] Small molecules interact with DNA primarily by three binding modes: electrostatic binding, groove binding and intercalative binding (Fig. 1),[8–10] which can be tested by spectroscopy, electrochemical analysis, viscosity measurement and gel electrophoresis. Electrostatic binding is the interaction between cationic species and the negatively charged DNA phosphate backbone. It occurs along the external DNA double helix and does not possess selectivity. In groove binding, interactions with the two grooves of the DNA double helix generally involve direct hydrogen bonding or van der Waals interactions with the nucleic acid bases in the deep major groove or the wide shallow minor groove of the DNA helix. Intercalative binding is stronger than the other two binding modes because the surface of intercalative molecule is sandwiched between the aromatic, heterocyclic base pairs of DNA.[11] Intercalative binding leads to the melting chain and elongation of the DNA double helix, which is an important feature of intercalative binding. Also, the hypochromicity and red shift in the absorption spectra of complexes indicate the intercalative interaction between complexes and DNA bases.[12–14]

Salicylic acid (Hsal) can easily form a stable complex with the metal ion. A large number of studies confirmed that metal complexes with salicylic acid have higher biological activity and lower toxicity than that of isolated Hsal.[15] The antibacterial activities of the ternary lanthanide complexes with Hsal and the second ligand (such as 1,10-phenanthroline (phen), 8-hydroxyquinoline) are expected to be better than the lanthanide chloride or ligands.[16] Lanthanide ions with unique biological activity are becoming increasingly attractive within the chemical and pharmaceutical research field. The DNA binding of some lanthanides has been explored.[17] Synthesis and characterization of lanthanide complexes with Hsal and phen have been studied for their optical properties,[18] but little work has been done on their DNA binding properties. Furthermore, the relation between types of lanthanide complexes and their binding ability with DNA is still unclear.[19]

Here, 12 lanthanide complexes RE(sal)$_3$phen (RE^{3+} = La^{3+}, Pr^{3+}, Nd^{3+}, Sm^{3+}, Eu^{3+}, Gd^{3+}, Tb^{3+}, Dy^{3+}, Ho^{3+}, Tm^{3+}, Yb^{3+}, Lu^{3+}) were synthesized, and we used UV–visible spectra, fluorescence spectra and viscosity measurements to explore the interaction between RE(sal)$_3$phen complexes and ct-DNA. Our results provided evidence that the interaction mode between the complexes and DNA are intercalation binding.[20] Furthermore, the binding constant (K_b) and fluorescence quenching constant

* *Correspondence to: Yong-Liang Zhao, College of Chemistry and Chemical Engineering, Inner Mongolia University, Huhhot, 010021, China. Email: hxzhaoyl@163.com*

College of Chemistry and Chemical Engineering, Inner Mongolia University, Huhhot 010021, China

Applied Organometallic Chemistry

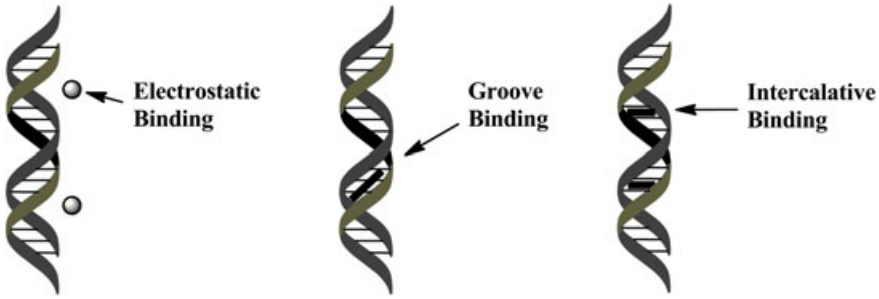

Figure 1. Illustration of electrostatic groove and intercalative binding of small molecules to the DNA double helix.

(K_q) were calculated, and a negative correlation between K_b or K_q and the lanthanide ion radius was found. Antibacterial activities of the 12 complexes were also investigated and we found that the antibacterial activities of the heavy rare earth complexes were better than those of light rare earth complexes. These findings may be helpful in understanding the mechanism of the interactions between DNA and lanthanide complexes. Also, they should be useful for the development of potential probes for DNA structure and new therapeutic reagents for tumours and other diseases.

Experimental

Materials and Instrumentation

Calf thymus DNA (ct-DNA, Sigma Chemical Co., USA), tris (hydroxymethyl) aminomethane hydrochloride (Tris–HCl) and ethidium bromide (EB) were used as received. Purity of salicylic acid and 1,10-phenanthroline (Sinopharm Chemical Reagent Co., China) was 99.5%. Purity of rare earth oxides were 99.99%. Other reactants and solvents were of analytical grade.

Elemental analysis (C, N and H) were performed with a Vario EL cube elemental analyser. The contents of rare earth elements were determined by ethylenediaminetetraacetic acid (EDTA) titration. Molar conductivity was measured on a DDS-11A conductivity meter with a DJS-I platinum black electrode at 25°C using *N*,*N*-dimethylformamide (DMF) as solvent, and the concentrations of complexes were 1.0×10^{-3} mol l^{-1}. IR spectra were obtained on a Nicolet Nexus 670 FT-IR spectrophotometer in the range 4000–500 cm^{-1}. Electrospray ionization (ESI) mass spectra were recorded on an LCQ Advantage MAX mass spectrophotometer with DMF as the proton source. Absorption spectra were recorded on a TU1901 spectrophotometer, using DMF as solvent, and the concentration of the complexes was 1.0×10^{-5} mol l^{-1}. Fluorescence spectra were carried out using a Shimadzu RF-5301PC spectrophotometer with excitation and emission slits of 10.0 nm at room temperature. Viscosity experiments were conducted on a Ubbelohde Viscomter at 25.0 ± 0.1°C.

Synthesis of RE(sal)$_3$phen

Preparation of $RECl_3$

RE_2O_3 was dissolved in concentrated HCl.[21] The mixture was heated until a crystallized film appeared above the solution, then cooled to room temperature. A powdered solid appeared, which was then dissolved in anhydrous ethanol to obtain 0.1 mol l^{-1} $RECl_3$ (RE^{3+} = La^{3+}, Nd^{3+}, Sm^{3+}, Eu^{3+}, Gd^{3+}, Dy^{3+}, Ho^{3+}, Tm^{3+}, Yb^{3+}) ethanol solution. The preparations of $TbCl_3$ and $PrCl_3$ ethanol solution were similar to other $RECl_3$ preparations except that H_2O_2 was added.

Synthesis of RE(sal)$_3$phen

Hsal (1.5 mmol) was dissolved in 5 ml ethanol, and aqueous ammonia was added to adjust the pH level to 7.0. An $RECl_3$ (0.5 mmol) solution was then added dropwise to the solution under stirring at 60°C. After reaction for 1 h, 0.50 mmol phen dissolved in 5 ml ethanol was added dropwise to this mixture under stirring for a further 2 h at 60°C. The precipitate was filtered out, washed twice with ethanol and dried at 50°C for several hours to obtain the product of RE(sal)$_3$phen.

[La(sal)$_3$phen] Anal. Calcd (%) for $LaC_{33}H_{23}O_9N_2$: C 54.26, H 3.17, N 3.84; Found: C 54.48, H 3.01, N 4.21. ESI-MS (DMF), *m/z*: 632.03, 739.07, 773.21, 845.89.

[Pr(sal)$_3$phen] Anal. Calcd (%) for $PrC_{33}H_{23}O_9N_2$: C 54.11, H 3.17, N 3.82; Found: C 54.67, H 3.28, N 3.61. ESI-MS (DMF), *m/z*: 633.87, 740.83, 775.09, 847.61.

[Nd(sal)$_3$phen] Anal. Calcd (%) for $NdC_{33}H_{23}O_9N_2$: C 53.87, H 3.15, N 3.81; Found: C 54.21, H 3.36, N 3.78. ESI-MS (DMF), *m/z*: 636.18, 744.03, 778.32, 848.70.

[Sm(sal)$_3$phen] Anal. Calcd (%) for $SmC_{33}H_{23}O_9N_2$: C 53.42, H 3.12, N 3.78; Found: C 52.95, H 3.07, N 4.30. ESI-MS (DMF), *m/z*: 644.93, 751.82, 786.00, 858.37.

[Eu(sal)$_3$phen] Anal. Calcd (%) for $EuC_{33}H_{23}O_9N_2$: C 53.31, H 3.12, N 3.77; Found: C 53.41, H 3.02, N 4.12. ESI-MS (DMF), *m/z*: 645.94, 752.84, 787.03, 859.60.

[Gd(sal)$_3$phen] Anal. Calcd (%) for $GdC_{33}H_{23}O_9N_2$: C 52.93, H 3.10, N 3.74; Found: C 52.58, H 3.39, N 4.27. ESI-MS (DMF), *m/z*: 650.93, 757.80, 791.98.

[Tb(sal)$_3$phen] Anal. Calcd (%) for $TbC_{33}H_{23}O_9N_2$: C 52.81, H 3.09, N 3.73; Found: C 52.81, H 3.09, N 3.73. ESI-MS (DMF), *m/z*: 651.94, 758.83, 793.03.

[Dy(sal)$_3$phen] Anal. Calcd (%) for $DyC_{33}H_{23}O_9N_2$: C 52.56, H 3.07, N 3.72; Found: C 52.14, H 3.22, N 4.12. ESI-MS (DMF), *m/z*: 656.99, 762.90, 798.08.

[Ho(sal)$_3$phen] Anal. Calcd (%) for $HoC_{33}H_{23}O_9N_2$: C 52.40, H 3.06, N 3.70; Found: C 52.66, H 2.94, N 4.16. ESI-MS (DMF), *m/z*: 657.96, 764.82, 799.08.

[Tm(sal)$_3$phen] Anal. Calcd (%) for $TmC_{33}H_{23}O_9N_2$: C 52.12, H 3.05, N 3.68; Found: C 52.26, H 2.94, N 4.09. ESI-MS (DMF), *m/z*: 661.96, 768.79, 803.09.

[Yb(sal)$_3$phen] Anal. Calcd (%) for $YbC_{33}H_{23}O_9N_2$: C 51.84, H 3.03, N 3.66; Found: C 51.69, H 2.81, N 4.03. ESI-MS (DMF), *m/z*: 773.93, 808.11.

[Lu(sal)$_3$phen] Anal. Calcd (%) for $LuC_{33}H_{23}O_9N_2$: C 51.71, H 3.02, N 3.65; Found: C 51.27, H 2.84, N 4.04. ESI-MS (DMF), *m/z*: 774.81, 809.10.

Preparation of ct-DNA Solution and EB Solution

Ct-DNA was used without further purification, and its stock solution was prepared by dissolving appropriate solid DNA into doubly distilled water and storing at 4°C. The concentration of DNA in stock solution was determined by UV absorption at 260 nm using a molar absorption coefficient $\varepsilon_{260} = 6600$ l mol^{-1} cm^{-1}.[22] Purity of the DNA was checked by monitoring the ratio of the absorbance at 260–280 nm. The solution gave a ratio of A_{260}/A_{280} of 1.8–2.0, indicating that DNA was sufficiently free from protein.[23] Stock solutions of the complexes (1.0×10^{-3} mol l^{-1}) were prepared by dissolving in DMF and diluting to 1.0×10^{-5} mol l^{-1} with double-distilled water. EB stock solution was prepared by dissolving it in double-distilled water according to a ratio of $C_{DNA}/C_{EB} = 20$.

Test of Antibacterial Activity

Antibacterial activity of the ligands and the complexes against *Escherichia coli* was studied using the filter paper scraps diffusion method.[24,25] Small sterile filter papers of 6 mm diameter were prepared for the purpose of making bacteriostatic slices. The *E. coli* was spread on sterile Luria–Bertani (LB) agar plates using a sterile cotton swab. The 6 mm diameter sterile filter papers were coated with a 20 μl solution of Hsal, phen and the 12 complexes in DMF, respectively, and were then carefully placed at the centre of the lawn without touching the other parts and incubated at 37°C for 16–18 h. The inhibition zone around the film was then photographed and measured with a vernier caliper to evaluate the antibacterial performance. All experiments were carried out in parallel three times, and the average diameter values were calculated.

Results and Discussion

Composition Analysis and Molar Conductivity

The results of elemental analyses and rare earth EDTA titration indicated that the compositions of the complexes were RE(sal)$_3$phen (RE^{3+} = La^{3+}, Pr^{3+}, Nd^{3+}, Sm^{3+}, Eu^{3+}, Gd^{3+}, Tb^{3+}, Dy^{3+}, Ho^{3+}, Tm^{3+}, Yb^{3+}, Lu^{3+}). All the complexes were stable in air and easily dissolved in DMF and DMSO but difficult to dissolve in water, ethanol and acetone. The molar conductance values of lanthanide complexes in DMF are in the range 2.0–5.7 (S cm^2 mol^{-1}). These low values indicate that only a small fraction of lanthanide complexes ionize in DMF and these complexes are non-electrolytes.[26,27]

Thermogravimetry–Differential Scanning Calorimetry (TG-DSC)

Thermal decomposition of the complexes was studied using the TG technique, which can be regarded as an adjunct for speculating the composition of complexes. It can be found that the thermal behaviour of the 12 complexes is quite similar. The experiment was performed under air atmosphere with a heating rate of 10°C min^{-1}. The TG-DSC curves of Tm(sal)$_3$phen are shown (supporting information, Fig. S1) to be in the range 30–700°C. As shown in Fig. S1, the complex begins to decompose at about 180°C with obvious weight loss. The weight loss of the complex Tm(sal)$_3$phen around 180–320°C was 23.05%, which could be assigned to the complex with loss of one phen (the theoretical value is 23.70%). The weight loss of 41.48% at 320–640°C is consistent with the complex that loses three sal$^-$ with two COO$^-$ subtracted (the theoretical value is 42.51%). This result is in accordance with the composition of complexes predicted by elemental analyses, IR spectra and mass spectral data.

IR Spectra

The IR spectra of ligands phen, Hsal and all the obtained complexes were determined in the range 4000–500 cm^{-1}, some of which are given in Fig. S2. The spectra of the 12 lanthanide complexes are similar, which indicates that the complexes have a similar structure. As shown in Fig. S2(a), the bands at 3000–3500, 1659 and 1483 cm^{-1} could be attributed to the $\nu_{(O\text{-}H)}$(COOH) stretching vibration, $\nu_{(C=O)}$(COOH) vibration and $\delta_{O\text{-}H}$ (phenol) rocking vibration of Hsal.[27,28] After the formation of the complexes, those absorption peaks all disappeared except the peak of $\delta_{O\text{-}H}$ (phenol). Meanwhile, two new peaks appeared at 1596 and 1389 cm^{-1}, which could be assigned to the antisymmetric and symmetric stretching vibrations of the carboxylate group, respectively. These changes indicate that the carboxylate ions of Hsal coordinate with the lanthanide ions in the complexes. Evidence of chemical bond formation between Tb^{3+} ions and the nitrogen atoms was confirmed as the vibrational band at 1640, 1587, 852 cm^{-1}, assigned to C=C, C=N and CH out-of-plane deformation[29] in the phenanthroline spectrum, shifted to 1623, 1552 and 841 cm^{-1} in the RE(sal)$_3$phen complexes, respectively. This indicates that nitrogen atoms of phenanthroline are coordinating RE^{3+} in complexes.[30]

The structures of the lanthanide complexes with salicylic acid have been discussed by several groups.[31,32] Burns and Baldwin have reported the crystal structure of samarium salicylate, which indicates that both the carboxylic and the phenolic oxygen atoms participate in the coordination with central lanthanide ions. In our work, $\delta_{O\text{-}H}$ (phenol) of Hsal shows almost no change after the formation of RE(sal)$_3$phen, which suggests that only the carboxylic participated in the coordination with RE^{3+}. Generally, the coordination number of RE ions in organic complexes is reported to be between 6 and 9. The structure of Tb(sal)$_3$phen has been predicted by Kaur.[33] On the basis of these previous reports and our above analysis (elemental analyses, IR spectra and ESI mass spectral data), the most suitable molecular structure of the complex is shown in Fig. 2. The coordinate number of the central metal ion was 8. The metal ion bonded to a chelating bidentate phen and three bidentate carboxyl groups from Hsal ligands.

Fluorescence Spectral Studies of DNA Binding

The binding of the complexes to ct-DNA has been studied by the fluorescence spectral method. EB is one of the most sensitive fluorescence probes; it can intercalate into DNA and the

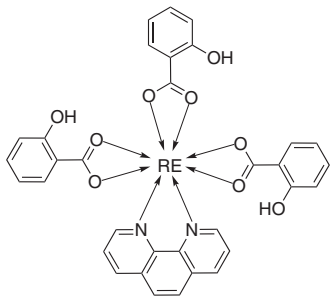

Figure 2. Predicted structure of the RE(sal)$_3$phen complex.

fluorescence of EB can be effectively increased. The metal complexes may replace EB in the binding to DNA, thus decreasing the emission intensity of EB. A quantitative solution (1.0 ml 1.0×10^{-5} mol l^{-1} DNA and 1.0 ml 5.0×10^{-7} mol l^{-1} EB) was titrated with increasing amounts of lanthanide complex (1.0×10^{-3} mol l^{-1}, 10 μl each time). As shown in Fig. 3, the fluorescence intensity of EB-DNA was quenched steadily with increasing concentration of $Tb(sal)_3phen$. We selected 537 nm as the excitation wavelength and recorded the emission spectra from 570 to 630 nm. A remarkable fluorescence decrease of the EB-DNA system was observed around the fluorescence peak at 592 nm. This indicates that the complex displaces EB from its binding sites, which leads to a large decrease in the emission intensity of the EB-DNA system. The fluorescence quenching of EB-DNA by complexes indicates the strong binding between DNA and the complex. Also, the interaction mode between the complexes and DNA is probably intercalation binding, which will be further validated by UV–visible absorption spectra and viscosity studies.

The quenching plots illustrate that the fluorescence quenching of EB-DNA by the complex is in good agreement with the linear Stern–Volmer equation[34]:

$$\frac{F_0}{F} = 1 + K_q[Q] \quad (1)$$

where F_0 is the emission intensity in the absence of quencher, F is the emission intensity in the presence of quencher, $[Q]$ is the quencher concentration, and K_q is the quenching constant. Taking $Tb(sal)_3phen$ for example, K_q is obtained from the slope of the F_0/F versus [DNA] linear plot (Fig. 3, inset) and is found to be 7.00×10^4 mol^{-1} l, which indicates a strong interaction of lanthanide complex with DNA. Plots of F_0/F versus $[Q]$ should appear to be linear. The illustration shows the Stern–Volmer quenching curve and data of the fluorescence quenching constant are presented in Table 1.

The fluorescence quenching of EB-DNA by complexes indicates that the complexes have a strong interaction with DNA. From the sequence of quenching constants of the complexes binding to EB-DNA, we can see that K_q is related to lanthanide ion radius, and the sequence of K_q is $Lu(sal)_3phen > Yb(sal)_3phen$ $Tm(sal)_3phen > Ho(sal)_3phen > Dy(sal)_3phen > Tb(sal)_3phen$

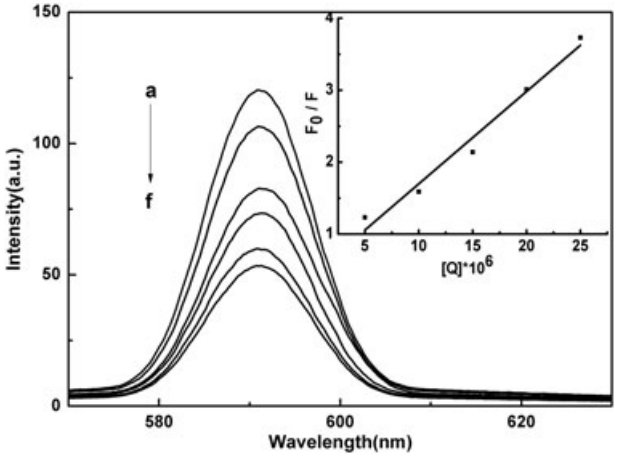

Figure 3. Effect of $Tb(sal)_3phen$ (1.0×10^{-3} mol L^{-1}, 10 μl each time) on the fluorescence spectra of EB-DNA system (1.0 ml 1.0×10^{-5} mol L^{-1} DNA and 1.0 ml 5.0×10^{-7} mol L^{-1} EB). $\lambda_{ex} = 537$ nm, $\lambda_{max-em} = 592$ nm. Arrow a → f shows the intensity changes upon increasing concentration of the complex. The inset plot shows the relative fluorescent intensity curve of $Tb(sal)_3phen$ interaction with EB-DNA.

Table 1. Fluorescence quenching constant of complex interaction with DNA

Complex	K_q (mol^{-1} l)
$La(sal)_3phen$	$(4.69\pm0.01)\times10^4$
$Pr(sal)_3phen$	$(6.13\pm0.01)\times10^4$
$Nd(sal)_3phen$	$(6.26\pm0.01)\times10^4$
$Sm(sal)_3phen$	$(6.46\pm0.01)\times10^4$
$Eu(sal)_3phen$	$(6.57\pm0.01)\times10^4$
$Gd(sal)_3phen$	$(6.87\pm0.01)\times10^4$
$Tb(sal)_3phen$	$(7.00\pm0.01)\times10^4$
$Dy(sal)_3phen$	$(7.08\pm0.01)\times10^4$
$Ho(sal)_3phen$	$(7.73\pm0.02)\times10^4$
$Tm(sal)_3phen$	$(9.01\pm0.01)\times10^4$
$Yb(sal)_3phen$	$(9.11\pm0.01)\times10^4$
$Lu(sal)_3phen$	$(1.14\pm0.01)\times10^5$

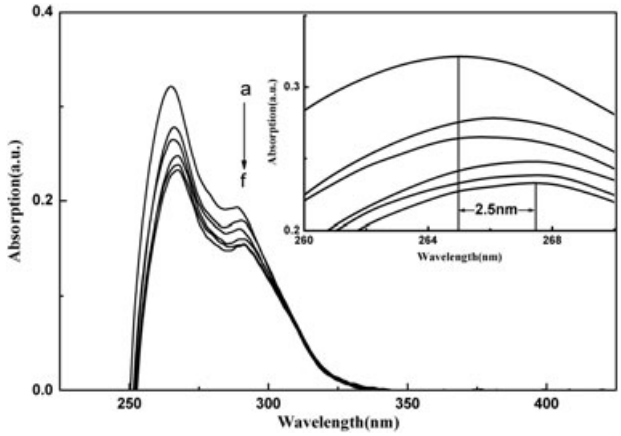

Figure 4. Absorption spectra of $Tb(sal)_3phen$ (2.00 ml 1.0×10^{-5} mol L^{-1}) in the presence of increasing amounts of ct-DNA ([DNA] = 0–0.476 μM, 0.01 mol l^{-1} Tris–HCl, pH 7.2) , 20 μl each time. Arrow a → f shows the absorbance changes upon increasing ct-DNA concentration.

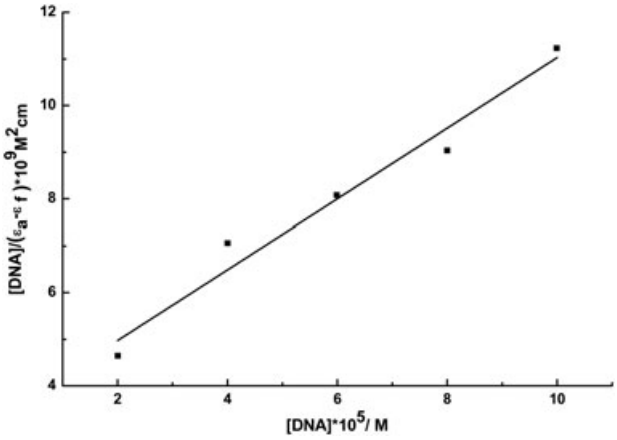

Figure 5. Pattern of $Tb(sal)_3phen$ of $[DNA]/(\varepsilon_f - \varepsilon_a)$ linear relation to [DNA].

Table 2. Binding constant of complex interaction with DNA

Complex	$Pr(sal)_3phen$	$Nd(sal)_3phen$	$Gd(sal)_3phen$	$Tb(sal)_3phen$	$Yb(sal)_3phen$
$K_b(mol^{-1}\ l)$	$(6.86 \pm 0.09) \times 10^3$	$(1.72 \pm 0.03) \times 10^4$	$(1.79 \pm 0.01) \times 10^4$	$(2.19 \pm 0.08) \times 10^4$	$(2.63 \pm 0.17) \times 10^4$

$Gd(sal)_3phen > Eu(sal)_3phen > Sm(sal)_3phen > Pr(sal)_3phen > Nd(sal)_3phen > La(sal)_3phen$. The data suggest that the binding ability of $Lu(sal)_3phen$ is strongest whose lanthanide ion radius is the smallest, and the binding ability of $La(sal)_3phen$ is weakest whose lanthanide ion radius is the largest. This may be the result of the effect of the trivalent lanthanide ion radius. The Lu^{3+} has the smallest radius, largest charge density and strongest electrostatic interaction with DNA in these complexes, so the capacity of phen in $Lu(sal)_3phen$ inserting into the base pairs of DNA is the strongest and the fluorescence quenching constant is the largest.[35] Conversely, the capacity of $La(sal)_3phen$ inserting into the base pairs is weakest and the fluorescence quenching constant is smallest. These data indicate that the K_q of the 12 complexes is inversely related to the lanthanide ion radius.

UV–Visible Absorption Spectral Studies of DNA Binding

The UV–visible absorption spectra of ligands phen, Hsal as well as all the complexes were determined in the range 200–400 nm. The UV–visible absorption spectra of the 12 lanthanide complexes are similar, and only that of $Tb(sal)_3phen$ is given. As shown in Fig. S3, the peak of phen is 265 nm in the lanthanide complex, which is similar to that of isolated phen (264 nm). The peak of salicylic acid at 297 nm shifted to 289 nm in the complex, which indicates that the lanthanide ion coordinated with salicylic acid.

The spectra of $Tb(sal)_3phen$ with increasing concentration of DNA are shown in Fig. 4. It can be seen that the absorption spectra showed obvious hypochromicity at an absorbance peak of 265 nm, together with a red shift of about 2.5 nm with increasing DNA concentration. The hypochromicity and red shift in the absorption spectra of complexes indicated the intercalative binding of complexes to DNA bases. This can be explained as follows. There is a strong interaction in the molecular stack between the DNA base pairs and the planar aromatic chromophore of the complexes.[36–38] An orbit coupling occurs between the empty π^*-orbital of the phen couples and the π^*-orbital of the DNA base pairs, which causes an energy decrease and a decrease of the π–π^* transition energy of the phen. Therefore, the absorption peak of the complexes around 265 nm exhibits a red shift. At the same time, the empty π^*-orbital is partially filled with electrons, reducing the π–π^* transition probability, which leads to hypochromism of the complexes.

In order to further illustrate the binding strength of the complexes, the intrinsic binding constant K_b was determined. K_b is a tool for investigating the magnitude of the binding strength of a compound bound to DNA and represents the binding constant per DNA base pair. It can be obtained by monitoring the changes in absorbance at the corresponding λ_{max} with increasing concentration of DNA and given by the ratio of slope to the *y* intercept in plots of [DNA]/(ε_a ε_f) versus [DNA], according to the following equation[39–43]:

$$\frac{[DNA]}{\varepsilon_a - \varepsilon_f} = \frac{[DNA]}{\varepsilon_b - \varepsilon_f} + \frac{1}{K_b(\varepsilon_b - \varepsilon_f)} \quad (2)$$

The binding constant K_b of the complex to ct-DNA is determined from equation (2), where [DNA] represents the concentration of DNA, and ε_a, ε_f and ε_b correspond to the apparent extinction coefficient A_{obsd}/[complex], the extinction coefficient for free complex and for the complex in the fully bound form, respectively. The binding constant K_b for $Tb(sal)_3phen$ has been determined from the plot of [DNA]/($\varepsilon_a - \varepsilon_f$) versus [DNA] (Fig. 5). The binding constants of some complexes are obtained in a similar way and shown in Table 2.

As shown in Table 2, the K_b values were calculated to be from 6.86×10^3 to 2.63×10^4 M^{-1}, suggesting a relatively strong binding of $RE(sal)_3phen$ complexes with DNA. The K_b values obtained for the complexes are close to those of the so-called DNA-intercalative Ru(II) complexes (1.1×10^4–4.8×10^4 M^{-1}),[44,45] but they are much lower than that of the classical intercalator, ethidium bromide(10^7 M^{-1}). Also, the sequence of binding ability of the complexes to DNA is $Yb(sal)_3phen > Tb(sal)_3phen > Gd(sal)_3phen > Nd(sal)_3phen > Pr(sal)_3phen$. This suggests that K_b is also related to the lanthanide ion radius, which is consistent with the fluorescence quenching constant K_q. It may be concluded that the complexes bind to DNA mainly in intercalation mode.

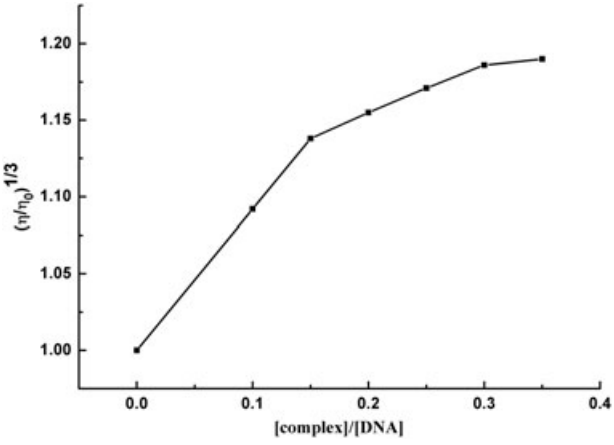

Figure 6. Influence on DNA viscosity at different concentrations of $Gd(sal)_3phen$. η_0 and η are the relative viscosity of DNA solution before and after the addition of complexes, respectively. $C_{DNA} = 1.00 \times 10^{-4}$ mol l^{-1}.

Table 3. Diameters of antibacterial rings of complexes with different concentrations on *E. coli* mm^{-1}

Compound	Concentration (mol l^{-1})		
	0.004	0.008	0.012
DMF	<10	<10	<10
Hsal	<10	<10	<10
Phen	<10	<10	13.8
$Pr(sal)_3phen$	16.8	17.8	23.5
$Nd(sal)_3phen$	17.5	18.5	23.2
$Gd(sal)_3phen$	17.3	18.7	23.7
$Tb(sal)_3phen$	17.8	19.1	24.5
$Tm(sal)_3phen$	18.4	19.7	24.7
$Yb(sal)_3phen$	18.5	20.0	24.8

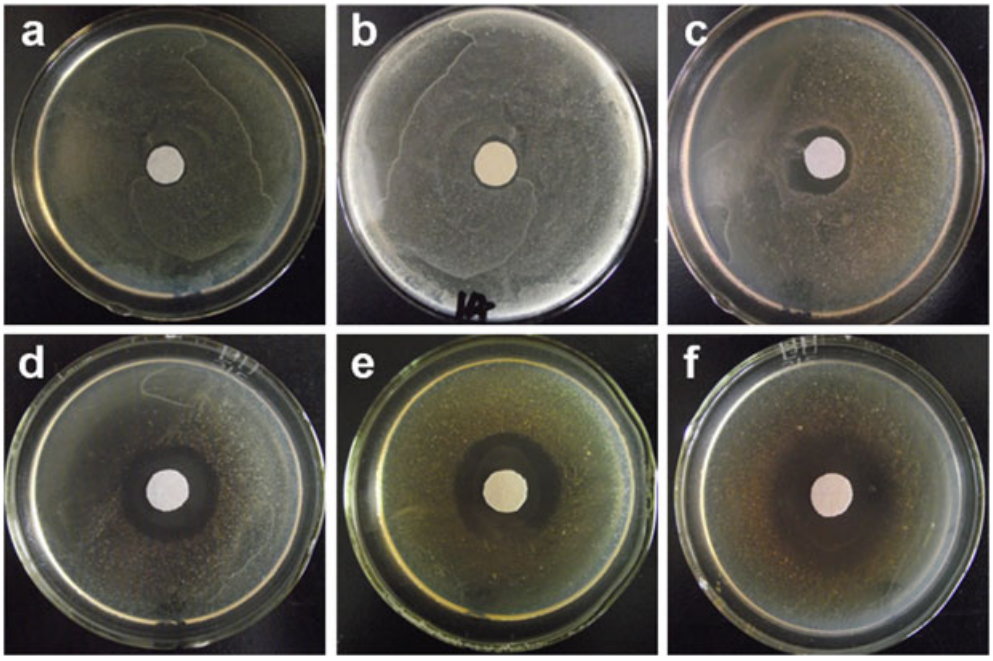

Figure 7. Antibacterial rings of (a) 0.012 mol l^{-1} DMF, (b) 0.012 mol l^{-1} Hsal, (c) 0.012 mol l^{-1} phen and $Yb(sal)_3phen$ at different concentrations on *E. coli*: (d) 0.004 mol l^{-1}, (e) 0.008 mol l^{-1}, (f) 0.012 mol l^{-1}.

Viscosity Measurements

Viscosity studies were carried out in order to further investigate whether the interactions between DNA and lanthanide complex involve intercalation. The viscosity measurements of DNA are regarded as the least ambiguous and the most critical test of a binding model in solution in the absence of crystallographic structural data.[46,47] A classical intercalation model is known to cause a significant increase in the viscosity of a DNA solution due to an increase in lengthening in the DNA helix. Furthermore, non-classical intercalation (partial intercalation) of the complex would reduce the DNA viscosity, and the non-intercalation binding (such as electrostatic binding and groove binding) causes no obvious change of DNA viscosity.[48,49] As shown in Fig. 6, the relative viscosity of the DNA solution was enhanced with increase in $Gd(sal)_3phen$. Such behaviour further suggests that the major interaction mode between $Gd(sal)_3phen$ and DNA should be intercalation binding. This may be caused by complexes that exhibit a strong tendency to interact with DNA. The increasing viscosity profile indicates that the complexes are effective intercalators.

Antibacterial Activities of Ligands and Complexes

The ligands and complexes were evaluated by the filter paper scraps diffusion method against *E. coli*. A large diameter of the inhibition zone indicates stronger antibacterial activity of a complex. As shown in Table 3 and Fig. 7, all the complexes exhibited stronger inhibitory effect on *E. coli* than the ligands. The antibacterial activities of the lanthanide complexes increased with increasing concentration of the complexes in the range 0.004–0.012 mol l^{-1}. A complex is usually considered to have a strong inhibitory effect when the inhibition zone diameter is more than 20 mm and, as we can see from Table 3, all these complexes exhibit excellent antibacterial ability against *E. coli* when the concentration was 0.012 mol l^{-1}. Furthermore, the antibacterial activities of heavy rare earth complexes are stronger than those of the light rare earth complexes. The enhanced antibacterial activities of the complexes presumably result from the increase in liposolubility of the lanthanide complexes by the chelate effect.[23,50–52]

Conclusions

Twelve ternary lanthanide complexes $RE(sal)_3phen$ were prepared. Fluorescence quench, hypochromism studies and viscosity measurements suggest that the complexes exhibit a strong interaction towards DNA via intercalative binding. In particular, both the quenching constant K_q and the binding constant K_b have a negative correlation with the lanthanide ion radius. In addition, all these complexes exhibit excellent antibacterial ability against *E. coli*, and the antibacterial activities of the heavy rare earth complexes are stronger than those of the light rare earth complexes. The systematic study of the binding mode of the 12 $RE(sal)_3phen$ complexes may provide useful information about the mechanism of anticancer drugs binding to DNA, and thus will be beneficial to the design of new lanthanide DNA binding agents.

Acknowledgements

The research work is supported by the National Natural Science Foundation of China (21161013), Natural Science Foundation of Inner Mongolia (2011MS0202), the Opening Foundation for Significant Fundamental Research of Inner Mongolia (2010KF03) and a fund from the Inner Mongolia University '211 project' innovative training project.

References

[1] R. Nagane, T. Koshigoe, M. Chikira, *J. Inorg. Biochem.* **2003**, *93*, 204–212.
[2] Y. B. Zeng, N. Yang, W. S. Liu, N. Tang, *J. Inorg. Biochem.* **2003**, *97*, 258–264.
[3] A. Silvestri, G. Barone, G. Ruisi, M. T. Lo Giudice, S. Tumminello, *J. Inorg. Biochem.* **2004**, *98*, 589–594.

[4] H. Mansouri-Torshizi, M. I-Moghaddam, A. Divsalar, A. A. Saboury, *Bioorg. Med. Chem.* **2008**, *16*, 9616–9625.
[5] B. K. Sahoo, K. S. Ghosh, R. Bera, S. Dasgupta, *Chem. Phys.* **2008**, *351*, 163–169.
[6] S. Rauf, J. J. Gooding, K. Akhtar, M. A. Ghauri, M. Rahman, M. A. Anwar, A. M. Khalid, *J. Pharm. Biomed. Anal.* **2005**, *37*, 205–217.
[7] H. Y. Zhang, H. J. Yu, J. S. Ren, X. G. Qu, *Biophys. J.* **2006**, *90*, 3203–3207.
[8] M. Khorasani-Motlagh, M. Noroozifar, S. Khmmarnia, *Spectrochim. Acta A* **2011**, *78*, 389–395.
[9] C. V. Kumar, E. H. Asuncion, *J. Am. Chem. Soc.* **1993**, *115*, 8541–8553.
[10] L. S. Lerman, *J. Mol. Biol.* **1961**, *3*, 18–30.
[11] L. S. Ling, Z. K. He, F. Chen, Y. E. Zeng, *Talanta* **2003**, *59*, 269–275.
[12] G. S. Manning, *Rev. Biophys.* **1978**, *11*, 179–246.
[13] M. Coll, C. A. Frederich, A. H. J. Wang, A. Rich, *Proc. Natl. Acad. Sci. U. S. A.* **1987**, *84*, 8385–8389.
[14] A. H. J. Wang, G. Ughetto, G. J. Quigley, A. Rich, *Biochemistry* **1987**, *26*, 1152–1163.
[15] I. Raskin, *Annu. Rev. Plant. Physiol. Plant. Mol. Biol.* **1992**, *43*, 439–463.
[16] D. F. Guo, J. He, Z. Z. Zeng, *J. Chin. Rare Earth* **2004**, *22*, 55–60.
[17] C. L. Tong, X. J. Zhuo, Y. Guo, Y. H. Fang, *J. Lumin.* **2010**, *130*, 2100–2105.
[18] C. J. Xu, *J. Hangzhou Teach. College (Nat. Sci. Ed.)* **2004**, *3*, 281–284.
[19] Y. C. Liu, K. J. Zhang, R. X. Lei, J. N. Liu, T. L. Zhou, Z. Y. Yang, *J. Coord. Chem.* **2012**, *65*, 2041–2054.
[20] X. Li, Y. H. Peng, X. G. Qu, *Nucleic Acids Res.* **2006**, *34*, 3670–3676.
[21] C. H. Huang, Rare Earth Coordination Chemistry, Science Press, Beijing, **1997**.
[22] C. Z. Huang, Y. F. Li, P. Feng, *Talanta* **2001**, *55*, 321–328.
[23] J. Marmur, *J. Mol. Biol.* **1961**, *3*, 208–218.
[24] M. F. Zhou, Q. Z. He, *J. Rare Earth* **2008**, *26*, 473–477.
[25] Y. M. Song, J. P. Xu, L. Ding, Q. Hou, J. W. Liu, Z. L. Zhu, *J. Inorg. Biochem.* **2009**, *103*, 396–400.
[26] M. D. Toylar, C. D. Carter, C. I. Wynter, *J. Inorg. Nucl. Chem.* **1968**, *30*, 1503–1511.
[27] W. J. Gear, *Coord. Chem. Rev.* **1971**, *7*, 81–122.
[28] Z. M. Wang, *Inorg. Chem.* **1995**, *11*, 308–312.
[29] B. Yan, Y. Y. Bai, *J. Fluoresc.* **2005**, *15*, 605–611.
[30] H. X. Wu, *J. Lumin.* **2006**, *27*, 270–274.
[31] D. A. Durham, F. A. Hart, *J. Inorg. Nucl. Chem.* **1969**, *31*, 145–157.
[32] J. H. Burns, E. H. Baldwin, *Inorg. Chem.* **1977**, *16*, 289–294.
[33] G. Kaur, Y. Dwivedi, S. B. Rai, *Mater. Chem. Phys.* **2011**, *130*, 1351–1356.
[34] J. R. Lakowicz, G. Webber, *Biochemistry* **1973**, *12*, 4171–4179.
[35] J. K. Barton, J. M. Goldberg, C. V. Kumar, N. J. Turro, *J. Am. Chem. Soc.* **1986**, *108*, 2081–2088.
[36] A. M. Pyle, J. P. Rehmann, R. Meshoyrer, C. V. Kumar, N. J. Turro, J. K. Barton, *J. Am. Chem. Soc.* **1989**, *111*, 3051–3058.
[37] E. C. Long, J. K. Barton, *Acc. Chem. Res.* **1990**, *23*, 271–273.
[38] S. A. Tysoe, R. J. Morgan, A. D. Baker, T. C. A. Strekas, *J. Phys. Chem.* **1993**, *97*, 1707–1711.
[39] C. V. Kumar, E. H. Asuncion, *J. Am. Chem. Soc.* **1993**, *115*, 8547–8553.
[40] V. G. Vaidyanathan, B. U. Nair, *J. Inorg. Biochem.* **2003**, *94*, 121–126.
[41] P. U. Maheswari, M. Palaniandavar, *Inorg. Chim. Acta* **2004**, *357*, 901–912.
[42] S. Kashanian, M. B. Gholivand, F. Ahmadi, A. Taravati, A. H. Colagar, *Spectrochim. Acta A* **2007**, *67*, 472–478.
[43] G. Psomas, A. Tarushi, E. K. Efthimiadou, *Polyhedron* **2008**, *27*, 133–138.
[44] X. H. Zou, B. H. Ye, H. Li, Q. L. Zhang, H. Chao, J. G. Liu, L. N. Ji, *J. Biol. Inorg. Chem.* **2001**, *6*, 143–150.
[45] A. M. Pyle, J. P. Rehmann, R. Meshoyrer, C. V. Kumar, N. J. Turro, J. K. Barton, *J. Am. Chem. Soc.* **1989**, *111*, 3051–3058.
[46] C. A. Mitsopoulou, C. E. Dagas, C. Makedonas, *Inorg. Chim. Acta* **2008**, *361*, 1973–1982.
[47] I. U. H. Bhat, S. Tabassum, *Spectrochim. Acta A* **2009**, *72*, 1026–1033.
[48] T. M. Kelly, A. B. Tossi, D. J. McConnell, T. C. A. Strekas, *Nucleic Acids Res.* **1985**, *13*, 6017–6034.
[49] S. Satyanarayana, J. C. Dabrowiak, J. B. Chaires, *Biochemistry* **1992**, *31*, 9319–9324.
[50] A. Chaudhary, S. Dave, R. K. Saini, R. V. Singh, *Main Group Met. Chem.* **2001**, *24*, 217–221.
[51] A. Chaudhary, N. Bansal, A. Gajraj, R. V. Singh, *J. Inorg. Biochem.* **2003**, *96*, 393–400.
[52] S. Priya, M. S. Balakrishna, J. T. Mague, S. M. Mobin, *Inorg. Chem.* **2003**, *42*, 1272–1281.

Supporting Information

Additional supporting information may be found in the online version of this article at the publisher's web-site.